

A Line Charge Model for Estimating Electric Charge Transfer
in Lightning Flashes

William Hawkins

April 25, 2017

Acknowledgements

I must thank many individuals for their help, assistance, and encouragement, without which this honors thesis would have been impossible to complete. First, thank you Dr. Chris Maggio for serving as my advisor, for all the guidance and support from the beginning of this project, for making working on this a great experience, and for the years of physics instruction in the classroom. I must also thank Dr. John Travis, Dr. Charles Ghany, for their willingness to serve on my committee, as well as Dr. Clinton Bailey for serving as the committee's honors representative. Along with those already mentioned, I would also like to thank Dr. Jerry Ballard, Dr. Tommy Leavelle, Mr. Daniel Watson, and Dr. David Magers for the stellar mathematics and science education experience that they have provided me through their instruction over the years. Additionally, I'd like to thank Dr. Thomas Marshall at the University of Mississippi for providing us with flat plate antenna data for our return stroke analysis.

I must also thank my parents Dana and Andy, my step-parents Jeff and India, my brothers John Andrew, Austin, and Jacob, and my grandparents, all of whom have always encouraged me to accomplish my goals in all areas of life. Finally, thank you to my friends Will, Taylor, Scotty, Jase, Ben, Nathan, Cade, Carson, Paul, Trey, Emily, Keegan, Lexi, Matt, and all the men of Shawreth. You have made my college years fantastic, and have helped me with this thesis in more ways than you will ever know.

Contents

1	Introduction	5
1.1	The Electrical Structure of Thunderstorms	5
1.2	Maggio's Distributed Model	9
2	Equipment	12
2.1	Electric Field Mills	12
2.2	Lightning Mapping Array and Lightning Detection and Ranging Network	13
2.3	Flat Plate Antenna	15
3	Model Derivation	16
3.1	Physical Background	16
3.2	Modeling the Charge Regions With a Line	19
3.3	Solving for Charge	20
3.4	Principal Components Analysis	22
4	Model Verification	25
5	Analysis of Individual Return Strokes	33
6	Conclusion	36
7	Appendix - Instructions for Operating the Program	39

List of Figures

1.1	A Simplified Model of an IC and CG Lightning Flash	6
2.1	A Field Mill at Kennedy Space Center	13
2.2	Example LMA Data from an IC Flash.	14
2.3	Identifying Polarity of Charge Regions using LMA Source Points	15
2.4	Electric Field Determined by Slow Antenna, at KSC Mill 14	15
3.1	A Line of Charge on the x-Axis, producing an E-Field at point P	18
3.2	Example of Image Line Charges.	20
3.3	Example PCA Orthogonal Regression	23
5.1	Electric Field Determined by Slow Antenna, at KSC Mill 14	34

List of Tables

4.1	Simulation Comparison Data.	27
5.1	Results of Individual Return Stroke Analysis	35

Chapter 1

Introduction

For hundreds of years, physicists have endeavored to understand and explain the natural phenomena of lightning. A particular question of interest to geophysicists is “how much charge is transferred in a lightning flash?” Attempts to answer this question have been ongoing since Wilson [1916] used rough estimates to quantify electric charge transfer. The underlying theory has remained the same, but modern instrumentation has allowed geophysicists to refine these estimates, especially due to the development of the electric field mill, flat plate antenna, Lightning Mapping Array, and the Lightning Detection and Ranging Network.

This paper presents a model that provides an estimate of the total electric charge transferred in a lightning flash, by treating the lightning channels as continuous lines of charge and employing instruments that inform us of the position of impulsive VHF radiation, along with measurements of the change in the electric field on the ground.

1.1 The Electrical Structure of Thunderstorms

A typical thundercloud has a main middle negative charge region and upper and lower positive charge regions above and below the negative charge region [Stolzenburg et al., 1998]. The buildup of charges in the thundercloud causes the cloud to exhibit behavior similar to a capacitor, and lightning flashes act to discharge this capacitor. In a lightning flash, there is movement of both positive and

negative charges between the charge regions of the cloud. Intracloud (IC) flashes transfer charge between the main negative and upper positive regions, with negative charge being deposited in the upper positive region, and an equal magnitude positive charge deposited in the main negative charge region [Shao and Krehbiel, 1996]. As the charge is transferred only between regions of the cloud, charge in the cloud is conserved. Cloud to Ground (CG) flashes transfer charge between the main negative region, lower positive region, and the ground. Negative polarity charge is deposited on the ground. Since charge is moved outside of the cloud, charge is not conserved within the cloud. The abrupt movement of charge between the charge regions produces a change in the electric field that can be measured on the ground. The change in electric field is due to the charges that were rearranged, so measurements of electric field change on the ground can be used to estimate the quantity of charge that was rearranged, or transferred in the flash. Figure 1.1 shows a simplified picture of the movement of charges in IC and CG flashes.

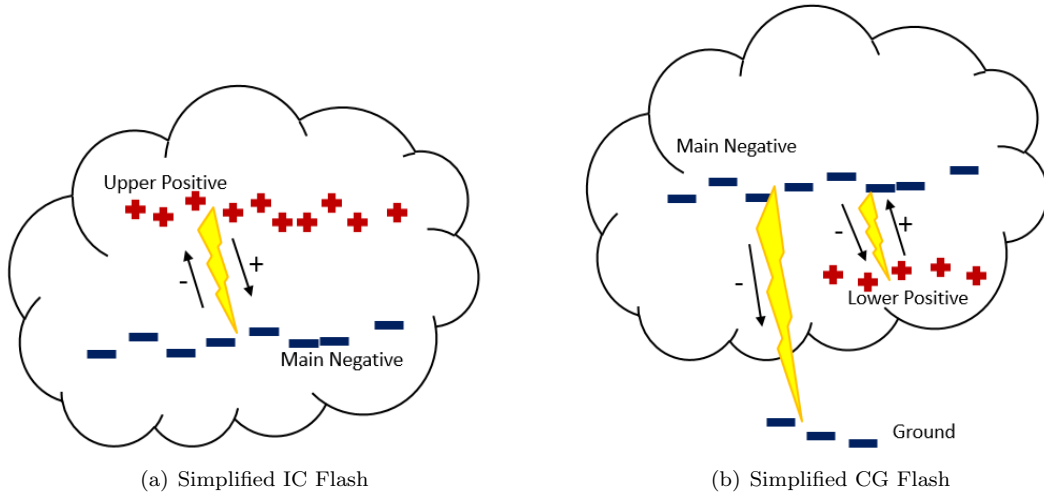


Figure 1.1: A Simplified Model of an IC and CG Lightning Flash

Investigations into these properties of lightning behavior began with Wilson [1916], who first demonstrated that charge transfer could be estimated using measurements of electric fields. Wilson supposed that the deposited charges could be modeled as point charges at the approximate locations of the cloud's charge distributions. As stated previously, in an CG flash, a negative charge is transferred to the ground. The transfer of negative charge to ground lowers the magnitude of

the main negative charge region, equivalent to adding an equal in magnitude positive charge to that region. The drop in measured electric field at the ground is due to this lowering of charge magnitude.

Wilson modeled such a transfer using a positive point charge approximately located in the region of the thundercloud where the discharge originated, with a height assumed to be 15 kilometers. He measured the change in electric field on the ground using “electrometers,” and he estimated the horizontal distance to the discharge by timing the time between the first electric field drop and the first hearing of thunder. Wilson assumed that, in CG flashes, the drop in measured electric field is equivalent to the electric field produced by the model’s positive point charge, which would be equal in magnitude to the charge lowered to ground. His model ignored any rearrangement of charges within the cloud. The charge transferred to ground could be approximated by finding the magnitude of the positive point charge that produces the modeled electric field that best fits the drop in measured electric field at the point of measurement.

Ultimately, using these very rough estimates, Wilson concluded that typical cloud to ground lightning flashes involve a transfer of about 30 Coulombs. He noted that the method was very difficult to use practically. Although Wilson’s work was rudimentary, his techniques, especially the Method of Images (described in detail in Section 3.2) and electric field measurements on the ground are echoed in subsequent investigations into atmospheric electricity.

Reynolds and Neill [1955] undertook experiments to attempt to determine an accurate figure for the positions of deposited charge in lightning flashes. They assumed that IC flashes could be modeled as a point charge dipole, with two equal point charges of opposite polarity. The positive dipole charge would be located in the cloud’s negative region and the negative dipole charge would be located in the cloud’s positive region. The modeled change in electric field was represented by:

$$\Delta E = \frac{2Q_- z_-}{[(x_- - x_1)^2 + (y_- - y_1)^2 + (z_-)^2]^{\frac{1}{2}}} - \frac{2Q_+ z_+}{[(x_+ - x_1)^2 + (y_+ - y_1)^2 + (z_+)^2]^{\frac{1}{2}}} \quad (1.1)$$

Where Q_- and Q_+ are the dipole charges, and $Q_- = -Q_+$. The positive charge Q_+ is at (x_+, y_+, z_+) and the negative charge Q_- is at (x_-, y_-, z_-) , while the electric field was measured at coordinate $(x_1, y_1, 0)$.

An array of seven electric-field measuring instruments could produce enough data to assign a

location to the position of the charge dipole and determine the total charge transferred in the lightning flash. The authors used trial and error to find values for the seven variables $Q, x_+, y_+, z_+, x_-, y_-, z_-$ that best matched the ΔE measurements at each measurement location. This was very difficult without computers, but they found that the negative dipole charge of an intracloud flash had an altitude of approximately 27,000 feet, the positive dipole charge had an altitude of approximately 25,000 feet, and total charge transfer ranged from 1 C up to 60 C. A particular limitation discussed was that “in some instances charge distributions apparently were so complex that the centers did not seem to satisfy the assumption of discrete spheres.” In other words, a single charge dipole was not a sufficient model for those charge distributions.

Jacobson and Krider [1976] performed a similar study in Florida on CG flashes, but used a computational method to perform a least squares statistical analysis. The computational method allowed them to statistically determine a best-fit solution to the point charge model using multiple measurements of the electric field in different locations at the time of a lightning flash. The measurement tools used by Jacobson and Krider consisted of an extensive network of over 20 field mills in the area surrounding Kennedy Space Center. Their results found that Florida CG flashes typically involve a charge transfer between 10 to 40 Coulombs.

The development of the VHF time of arrival Lightning Mapping Array (LMA) and Lightning Detection and Ranging Network (LDAR), further discussed in Section 2.2, freed atmospheric scientists from having to use blind guesses for the locations of cloud charge distributions. The LMA and LDAR are 3D lightning location systems that determine the location of moving charges by measuring the time of arrival of VHF radiation from lightning flashes. The sources of this radiation are mapped in three dimensions and time.

Sonnenfeld et al. [2006] incorporated the Lightning Mapping Array into two models for IC flash charge transfer, his Lumped Charge Model and his Distributed Model. The Lumped Charge model treats the charge transferred along a lightning channel as being equivalent to that of a point charge at the tip of where the LMA signals the terminus of a lightning channel with an equal but opposite polarity charge at the point where the LMA signals the beginning of the channel. In the distributed model, this transfer of charge is treated as being equivalent to charges at each LMA source point that appears along the channel rather than just the beginning and ending LMA channel point. These

models attempted to account for the time dependent change in measured electric field using the LMA to map the path of the lightning flash in real time.

Koshak et al. [2007] developed a model that employs a “dimensionality reduction” technique to help solve methods like that of Jacobson and Krider [1976]. In particular, the authors minimize the residual errors in an overdetermined system of equations as they iteratively converge to a solution for the positions and charges for the charge dipole left by the flash. Their model is typically employed for situations where there are no LMA or LDAR measurements, like Jacobson and Krider [1976] and Reynolds and Neill [1955]. However, the authors provide examples where they employ a LDAR system, and average the coordinates for each charge distribution to find a “center of charge” which they use for the coordinates for the dipole in their model. Vickers [2010] employed this model with LDAR and fast antenna data from three Florida lightning flashes at Kennedy Space Center to analyze individual return strokes produced by CG flashes. She concluded that, for the three flashes analyzed, that each return stroke transferred between a lower bound of 2.6 C up to an upper bound of 34 C. These results were in accordance with previous analysis of individual return strokes.

1.2 Maggio’s Distributed Model

Maggio [2007] investigated flashes from Langmuir Laboratory in New Mexico and their associated LMA data. His Distributed Charge Model treated the effect of charge transfer as being equivalent to point charges of appropriate polarity, depending on the type of flash, at the LMA source points, similar to Sonnenfeld’s Distributed model. For example, in an IC flash, negative charge is deposited in the thundercloud’s upper positive charge region and positive charge is deposited in the cloud’s main negative region. Because charge is conserved, a charge of $-Q$ was assumed to be deposited in the upper positive region, and a charge $+Q$ is assumed to be deposited in the main negative region. The LMA points were analyzed, and grouped into regions that represented the presumed locations of either the upper positive or main negative regions (this process is further described in Section 2.2). The LMA source points associated with the deposition of negative charge were each assigned a point charge of magnitude $-Q/n$ Coulombs at those positions, where n is the total number of LMA source points in that region. Similarly, the LMA source points associated with the deposition

of positive charge were assigned a point charge of magnitude $+Q/m$, where m is the total number of LMA source points in the main negative region. Each assigned point charge also necessitated an image point charge of opposite polarity in the same horizontal position below the xy -plane, in accordance with the method of images.

Each assigned point charge and image charge produced an electric field, which can be calculated at any point by Coulomb's Law for electric field:

$$\vec{E} = \frac{Q}{4\pi\epsilon_0} \frac{\vec{r} - \vec{r}'}{|\vec{r} - \vec{r}'|^3} \quad (1.2)$$

where \vec{r} points to the location where the electric field was measured on the ground and \vec{r}' points to the assigned point charge. Each assigned point charge contributes to the modeled electric field at the ground. A computer program varies the charges placed on each assigned point charge in each charge distribution until the Chi-Squared error between modeled and measured electric field is minimized:

$$\chi^2 = \frac{1}{S} \sum_{i=1}^N \frac{(E_{mi} - E_{ci})^2}{(\sigma_i)^2} \quad (1.3)$$

Where S is the number of degrees of freedom (number of measurements minus number of unknowns), E_{mi} is the measured electric field change at site i , E_{ci} is the modeled electric field change at site i , and σ_i is the uncertainty in the measurement of E_{mi} . i is a variable that refers to each ground measurement site.

The value for Q that results in the minimization of the above equation is the approximate charge transferred in the flash. A tremendous amount of computing time was required to find a value for Q that resulted in a minimum of Equation 1.3. Also, there is the possibility that the LMA data does not completely reflect the continuous horizontal extent of the discharge. The major necessary improvement is increased computational efficiency while returning similar results. A second benefit would be a model that better captures more of the continuous nature of the lightning channels, rather than a set of discrete points.

The Maggio study contributed greatly to the body of data on lightning charge transfer. Over forty IC and CG flashes with associated LMA and electric field data, along with his simulation results, were added to the literature. We present resimulations of the Maggio flashes using our

model in Chapter 4.

Conn [2012] and Masson [2014], Mississippi College students, employed the Maggio model in investigations of Florida CG lightning flashes at Kennedy Space Center. Masson studied the charge transfer in two CG flashes, while Conn studied the charge transfer in individual CG return strokes using electric field data obtained from flat plate antennas.

Chapter 2

Equipment

Equipment used in the application of our model includes electric field mills, flat plate antennas, the Lightning Mapping (LMA), and the Lightning Detection and Ranging Network (LDAR).

2.1 Electric Field Mills

The electric field mill measures the vertical component of the electric field at some coordinate (x, y, z) on the ground. A field mill consists of a rotating shutter that shields electrodes on the instrument. The electric charge from a thundercloud above will induce charge on the electrodes, which is registered and converted into the electric field strength at the ground. Figure 2.1 is an example of a field mill used at Kennedy Space Center in Florida. The array at KSC has a total of 34 field mills [Jacobson and Krider, 1976; Masson, 2014], while Langmuir Lab in New Mexico has an array of 3 field mills [Maggio, 2007].

The surface of the earth is a conductor [Wilson, 1916], so below the surface $\vec{E}_{\text{below}} = 0$ [Griffiths, 2012]. The electrostatic boundary conditions are:

$$\begin{aligned}\vec{E}_{\parallel \text{ above}} - \vec{E}_{\parallel \text{ below}} &= 0 \\ \vec{E}_{\perp \text{ above}} - \vec{E}_{\perp \text{ below}} &= \frac{\sigma}{\epsilon_0}\end{aligned}\tag{2.1}$$

Figure 2.1: A Field Mill at Kennedy Space Center



$\vec{E}_{\text{below}} = 0$, so $\vec{E}_{\parallel \text{ below}} = 0$. This implies that

$$\vec{E}_{\parallel \text{ above}} = 0 \quad (2.2)$$

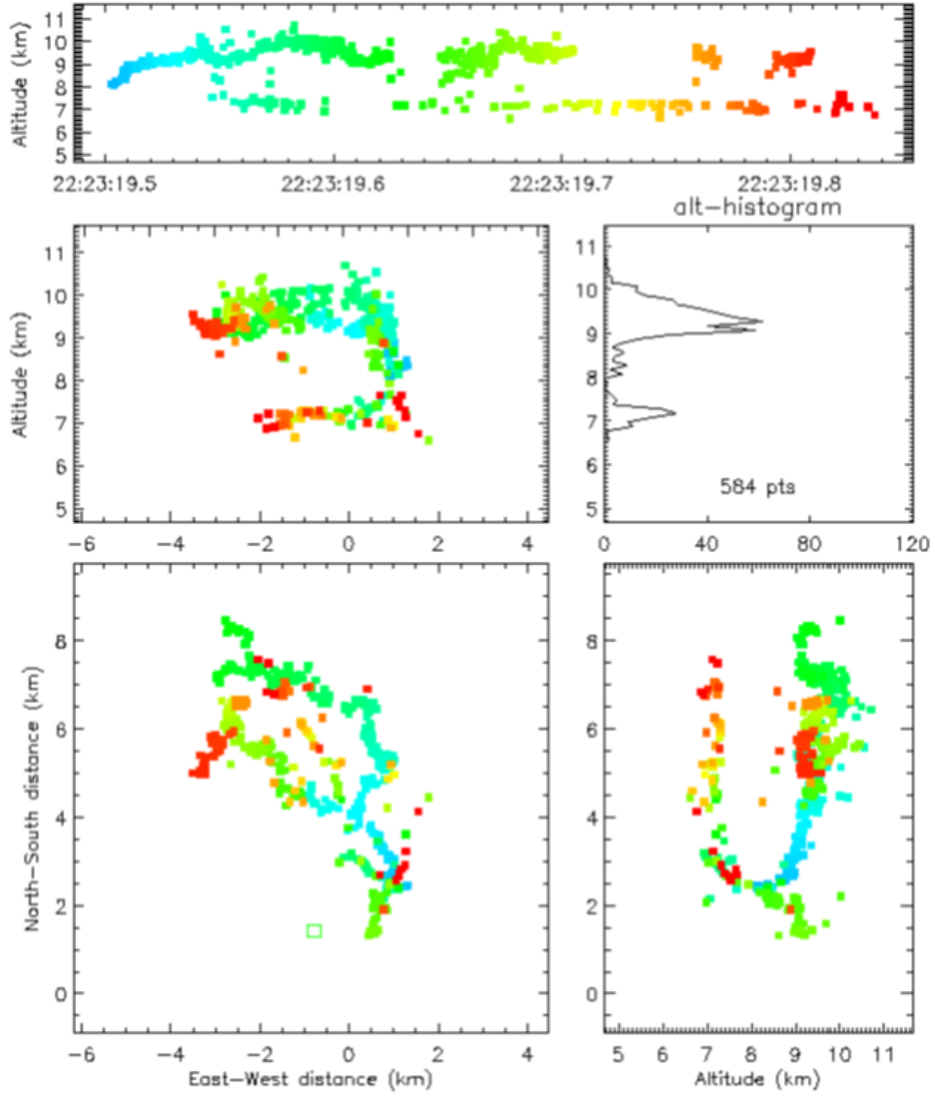
All of the electric field just above the conductor is therefore perpendicular to the surface of the conductor. Or, in our situation, all of the electric field at the earth's surface is in the z -direction.

2.2 Lightning Mapping Array and Lightning Detection and Ranging Network

The LMA is an instrument that provides the approximate locations of the movement of electrical charges in lightning flashes [Rison et al., 1999]. The LDAR operates in a similar manner. A result of lightning is the acceleration of electric charges, which produces electromagnetic radiation [Griffiths, 2012]. A network of antennas operating in VHF radio frequencies can receive this radiation, and can triangulate the position and time of the source of the radiation. Events that are detected by four or more stations can be traced to an (x, y, z) position and time.

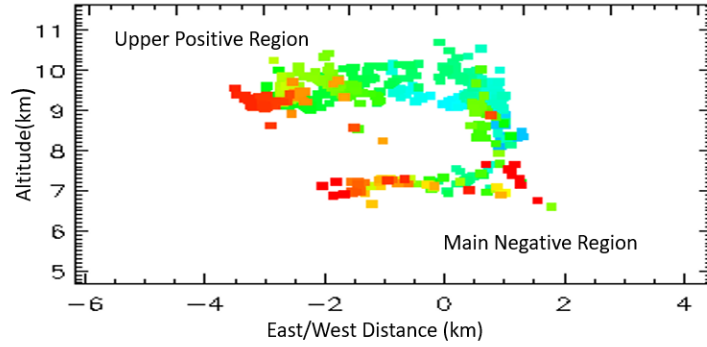
An LMA plot for an IC flash is provided in Figure 2.2. Note the separation of the charges by altitude. This separation makes the polarity of the charge region apparent. The dots at higher altitude are associated with negative charge being deposited into the upper positive region of the

Figure 2.2: Example LMA Data from an IC Flash.



cloud. Similarly, the LMA points with lower altitude are associated with the deposition of positive charge into the main negative cloud charge region. The deposition of negative charge produces more VHF radiation than the deposition of positive charge [Rison et al., 1999]. This allows us to identify the LMA points which refer to cloud charge regions of negative or positive polarity, as shown in Figure 2.3.

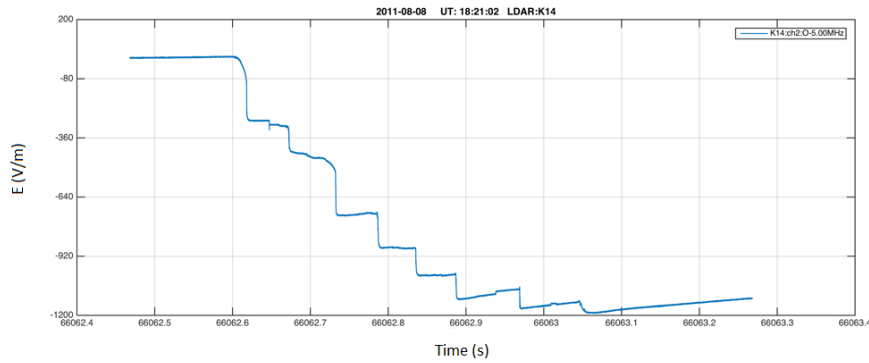
Figure 2.3: Identifying Polarity of Charge Regions using LMA Source Points



2.3 Flat Plate Antenna

The flat plate antenna is an instrument that, like the electric field mill, measures vertical electric field change at the ground [Maggio, 2007; Vickers, 2010]. But, the flat plate antenna has two settings, a slow setting and a fast setting. The “fast” setting collects data that appears as a sharp spike when triggered. The trigger could be a lightning flash or return stroke, subsequent connections to ground immediately following the initial CG flash. The “slow” setting records the continuous electric field at a high resolution that may show the electric field change due to intermittent charge transfers during a flash. An example plot from a flat plate antenna with the slow setting is shown in Figure 2.4. The sharp drops are the electric field changes due to individual return strokes (discussed further in Chapter 5).

Figure 2.4: Electric Field Determined by Slow Antenna, at KSC Mill 14



Chapter 3

Model Derivation

3.1 Physical Background

Electric charges exert a force on all surrounding charges [Griffiths, 2012]. Like charges repel, and opposite charges attract. This force is given by Coulomb's Law, where we can define vectors \vec{r}_1 , which points to the position of charge q_1 , and \vec{r}_2 which points to charge q_2 . Then the vector $\vec{r}_1 - \vec{r}_2$ points from q_1 to q_2 . The electric force acting from charge q_1 to charge q_2 is given by:

$$\vec{F} = \frac{1}{4\pi\epsilon_0} \frac{q_1 q_2 (\vec{r}_1 - \vec{r}_2)}{|\vec{r}_1 - \vec{r}_2|^3} \quad (3.1)$$

The electric field \vec{E} is defined to be the electric force per unit charge, due to charge Q . Given a charge q at a point, multiplying the value for \vec{E} at that point by the value of charge q will return the force that charge q experiences due to charge Q .

Let a vector \vec{r} be defined to point at the position in space where we wish to know the electric field, and let \vec{r}' be defined to point to the location of a charge Q , which is producing the electric field. The expression for the electric field due to a single point charge Q is:

$$\vec{E} = \frac{Q}{4\pi\epsilon_0} \frac{\vec{r} - \vec{r}'}{|\vec{r} - \vec{r}'|^3} \quad (3.2)$$

Now, what if we have an assortment of point charges, in some arrangement in space? Electric fields obey the principle of superposition, so if we add the electric field contributions from many charges at a point, we may discern the total electric field. For n point charges, each with charge q_i , and position in space \vec{r}_i , and a position where we wish to measure the field \vec{r} , the electric field is:

$$\vec{E} = \frac{1}{4\pi\epsilon_0} \sum_{i=1}^n \frac{q_i(\vec{r} - \vec{r}_i)}{|\vec{r} - \vec{r}_i|^3} \quad (3.3)$$

Now suppose we extend the above idea of multiple discrete point charges to a continuous system of charge, spread out evenly along a particular geometry. We might consider a line of charge, or a surface of charge, or a volume of charge, made up of tiny, infinitesimal pieces of charge, each a tiny dq , with an \vec{r}' pointing to each differential element of charge. Then the above sum becomes an integral over the whole geometry:

$$\vec{E} = \frac{1}{4\pi\epsilon_0} \int_S \frac{(\vec{r} - \vec{r}')dq}{|\vec{r} - \vec{r}'|^3} \quad (3.4)$$

Note that \vec{r}' is not a constant, it points to each dq on the charge distribution.

An important case for us to consider is the “line of charge,” placed on the x-axis, as in Figure 3.1. Then our $dq = \lambda dl$ where dl is a differential length on our line, and λ refers to the linear charge density, the number of coulombs of charge per meter of length, and if it’s constant: $\lambda = \frac{Q}{L}$.

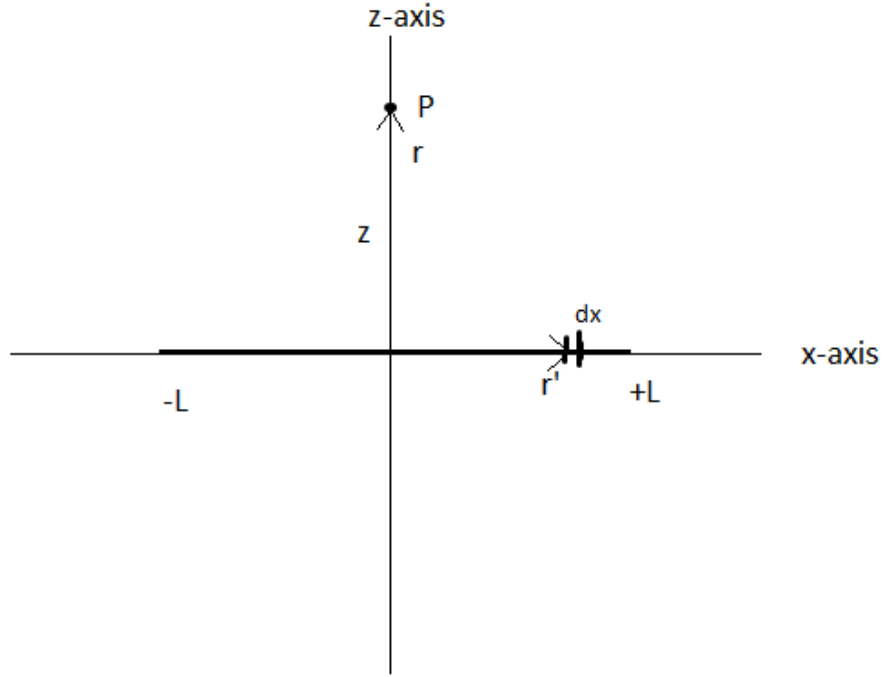
As an example, we will calculate \vec{E} for a line of charge of length $2L$ placed on the x-axis, measured at a point z above the middle of the line on the z-axis. We will substitute λdl for dq into the above equation. We define the vector $\vec{r}' = x\hat{x}$, and x lies between $-L$ and L . The point where we wish to measure the electric field is at some point z above the z-axis. This makes $\vec{r} = z\hat{z}$. The integral we must solve is:

$$\vec{E} = \frac{1}{4\pi\epsilon_0} \int_{-L}^L \frac{(z\hat{z} - x\hat{x})\lambda}{(x^2 + z^2)^{3/2}} dx \quad (3.5)$$

The \hat{x} portion of this integral is 0, because the horizontal contributions to the electric field will cancel each other out. So we’re left with:

$$\vec{E} = \frac{1}{4\pi\epsilon_0} \int_{-L}^L \frac{z\hat{z}}{(x^2 + z^2)^{3/2}} dx \quad (3.6)$$

Figure 3.1: A Line of Charge on the x-Axis, producing an E-Field at point P



Performing the integration, we find the solution to this integral is:

$$\vec{E} = \frac{z\lambda}{4\pi\epsilon_0} \left[\frac{x}{z^2\sqrt{x^2 + z^2}} \right]_{-L}^L \hat{z} \quad (3.7)$$

$$\vec{E} = \frac{1}{4\pi\epsilon_0} \frac{\lambda 2L}{z\sqrt{L^2 + z^2}} \hat{z} \quad (3.8)$$

This is, of course, the simplest case of the line of charge, but this example is crucial with regard to the subject of this paper. In our model, we must solve for the electric field due to lines of charge in arbitrary positions and orientations in space.

3.2 Modeling the Charge Regions With a Line

In previous studies of charge transfer in lightning flashes, the charge regions of the cloud have been represented by point charges [Wilson, 1916; Reynolds and Neill, 1955] or collections of point charges [Maggio, 2007]. While this gives a decent picture of the electrical structure of the cloud, as evidenced by the general agreement of results in previous experiments, one may pose the question whether this gives the best or most complete picture of the cloud's electrical structure.

As illustrated in the previous example, there are many different possible charge distributions that we might use to model the charge transfer of lightning flashes. If we use a line in 3-space to model the charge distribution, the equation for the line in vector form is:

$$\begin{aligned}\vec{r} &= (k_x t + x_0)\hat{x} + (k_y t + y_0)\hat{y} + (k_z t + z_0)\hat{z} \\ (t_i \leq t \leq t_f)\end{aligned}\tag{3.9}$$

Where k_x, k_y, k_z are constants that depend on the slope of the line, and (x_0, y_0, z_0) is an initial point. The collection of constants k_x, k_y, k_z is also called the "direction vector" of the line. t ranges across values that define the entirety of the line.

So if we let the above vector point to our charge distribution, and we let the vector $\vec{r} = r_x\hat{x} + r_y\hat{y} + r_z\hat{z}$ point to the position in space where we wish to measure the electric field, we can substitute \vec{r} and \vec{r} into an above equation and solve the integral:

$$\vec{E} = \frac{1}{4\pi\epsilon_0} \int_{t_i}^{t_f} \frac{\lambda ((r_x - (k_x t + x_0))\hat{x} + (r_y - (k_y t + y_0))\hat{y} + (r_z - (k_z t + z_0))\hat{z})}{[(r_x - (k_x t + x_0))^2 + (r_y - (k_y t + y_0))^2 + (r_z - (k_z t + z_0))^2]^{3/2}} dt \tag{3.10}$$

Now if we assume that λ is constant, that is, the charge is evenly distributed throughout the length of the line, so that $\lambda = \frac{Q}{L}$, this gets taken outside of the integral:

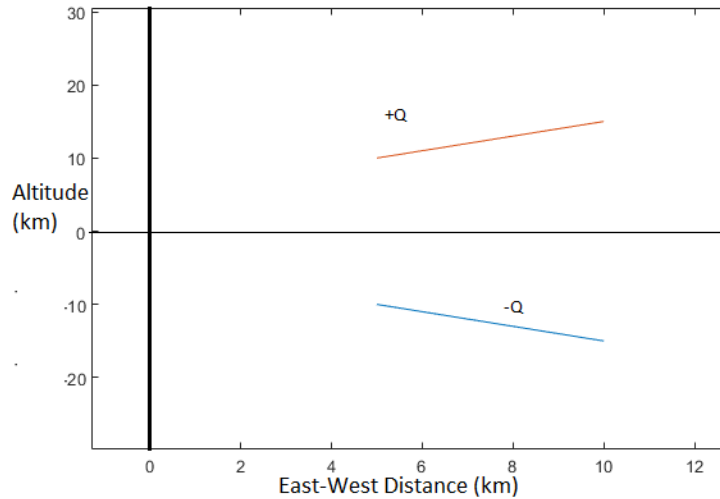
$$\vec{E} = \frac{Q}{4\pi\epsilon_0 L} \int_{t_i}^{t_f} \frac{(r_x - (k_x t + x_0))\hat{x} + (r_y - (k_y t + y_0))\hat{y} + (r_z - (k_z t + z_0))\hat{z}}{[(r_x - (k_x t + x_0))^2 + (r_y - (k_y t + y_0))^2 + (r_z - (k_z t + z_0))^2]^{3/2}} dt \tag{3.11}$$

The electric field meets the surface of a conductor at a right angle. The Earth is a conductor, which we assume takes the form of an infinite plane, so we are only concerned with the \hat{z} component of \vec{E} , because this is the perpendicular component to the conducting plane. We solve the integral

numerically.

Also because the surface of the Earth is a conducting plane with constant potential $V = 0$, we must use the method of image charges to calculate the electric field [Griffiths, 2012]. The method of images accounts for the enhancement of electric field due to the charge that is induced on the surface of the conductor. The method of images involves placing an equal in magnitude, but opposite in polarity charge on the direct opposite side of the conductor. The image charge has the effect of intensifying the electric field of the line charges above the conducting plane. Each line of charge in our model will have an mirror image line of opposite polarity charge placed below Earth's infinite conducting plane. An example of image line charges is shown in Figure 3.2. The top line charge is the real charge above Earth's surface, and holds a charge $+Q$ Coulombs. The bottom image line charge mirrors the real line of charge, and holds a charge $-Q$ Coulombs.

Figure 3.2: Example of Image Line Charges.



3.3 Solving for Charge

In our situation, we are not trying to solve expressions for electric fields. We have already measured electric fields using field mills, and we are trying to obtain a value for Q . Also, we aren't searching for just one Q , we have many measurements for \vec{E} , and may have many lines of charge in space that

we want to take into account. We are looking for a sequence of Q_1, Q_2, \dots, Q_n which, when placed on lines $1, 2, \dots, n$, produce the closest fit to the measured electric field, E_1, E_2, \dots, E_m . Linear algebra can help us find our charges.

To begin, for a system with n charge regions (lines) and m field mills, let A refer to the constants for the z-component of the electric field due to line of charge j and at field mill i . So we can say that $\vec{r}j$ points to line j and \vec{r} points to the position of field mill i , with $1 \leq i \leq m$, and $1 \leq j \leq n$. So for $A_{(i,j)}$:

$$A_{(i,j)} = \frac{1}{4\pi\epsilon_0 L} \int_{t_i}^{t_f} \frac{(r_{zi} - (k_{zj}t + z_{0j}))\hat{z}}{[(r_{xi} - (k_{xj}t + x_{0j}))^2 + (r_{yi} - (k_{yj}t + y_{0j}))^2 + (r_{zi} - (k_{zj}t + z_{0j}))^2]^{3/2}} dt \quad (3.12)$$

We perform a similar calculation for the image of the line of charge, and denote this quantity $B_{i,j}$. Then the total contribution to the electric field by line j at field mill i is:

$$\vec{E}(i, j) = Q_j A_{(i,j)} + (-Q_j) B_{(i,j)} \quad (3.13)$$

$$\vec{E}_{(i,j)} = Q_j (A_{(i,j)} - B_{(i,j)}) \quad (3.14)$$

Thus, by the principle of superposition, the electric field at field mill i produced by all of the lines in space is expressed by:

$$\vec{E}_i = Q_1(A_{(i,1)} - B_{(i,1)}) + Q_2(A_{(i,2)} - B_{(i,2)}) + \dots + Q_n(A_{(i,n)} - B_{(i,n)}) \quad (3.15)$$

If this is repeated for every field mill, we have a system of m equations in n unknowns. We would like to have $m > n$ so this becomes an overdetermined system of linear equations, for which we can find a least squares solution.

$$\begin{bmatrix} A_{(1,1)} - B_{(1,1)} & A_{(1,2)} - B_{(1,2)} & \dots & A_{(1,n)} - B_{(1,n)} \\ A_{(2,1)} - B_{(2,1)} & A_{(2,2)} - B_{(2,2)} & \dots & A_{(2,n)} - B_{(2,n)} \\ \dots & \dots & \dots & \dots \\ A_{(m,1)} - B_{(m,1)} & A_{(m,2)} - B_{(m,2)} & \dots & A_{(m,n)} - B_{(m,n)} \end{bmatrix} \begin{bmatrix} Q_1 \\ Q_2 \\ \dots \\ Q_n \end{bmatrix} = \begin{bmatrix} E_1 \\ E_2 \\ \dots \\ E_m \end{bmatrix} \quad (3.16)$$

We can call this system of equations $AQ = \vec{E}$. This system does not have a solution. But, there

are constraints we must place on Q_i that will converge the solution set to the closest possible physically realistic possibility. First, if Q_i refers to a region of negative polarity breakdown, Q_i must be less than zero. Similarly, if Q_i refers to a region of positive polarity breakdown, it must be greater than zero. Second, if the lightning flash in question is IC, then charge must be conserved, so we must only consider flashes where the total positive charge equals the total negative charge, so $Q_1 + Q_2 + \dots + Q_n = 0$. There are solvers built into MATLAB that allow us to search for solutions to the overdetermined linear system subject to these constraints.

This process of solving for the charge transfer required to produce the measured electric fields will work well, if we can draw lines in 3-space that correspond to the results of the flash’s LMA or LDAR data. However, the process of creating a ”best fit line” in 3D is not as obvious as in 2-space. As in Equation 3.9, a 3D line requires a direction vector (k_x, k_y, k_z) , an initial point (x_0, y_0, z_0) , and a range for $t \in [t_i, t_f]$. In 2D, we could just use linear regression, which finds a line that minimizes the error between the line and the points in the y-direction. If linear regression were carried out in 3D, we would have to minimize the error in the y- and z-directions and find a direction vector and t_i and t_f , which is not possible. We will have to employ an alternative.

3.4 Principal Components Analysis

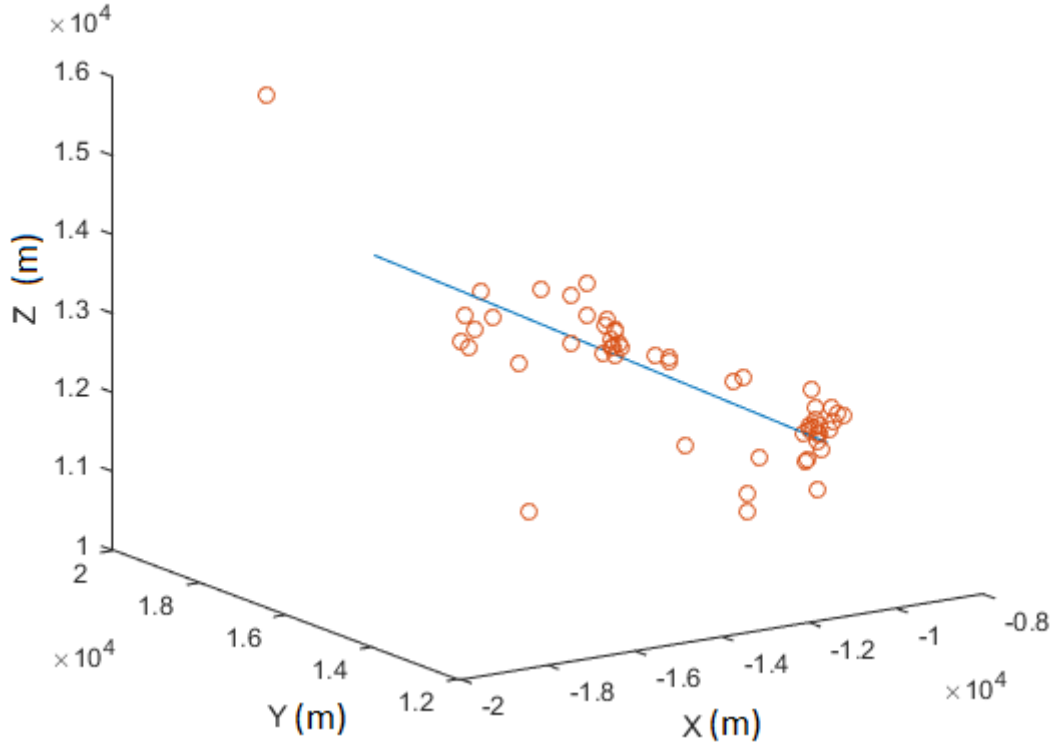
Principal Components Analysis (PCA) is a common technique for statistical analysis of large, multivariate data sets [Mathworks, 2015]. Its central idea is to “reduce the dimensionality of a data set consisting of a number of interrelated variables, while retaining as much as possible of the variation present.” This transforms the data to a new set of variables, which are the “principal components.”

The result is that p -dimensional observed data can be used to fit an r -dimensional hyperplane in p -dimensional space. The hyperplane has minimal orthogonal error from the data. For a hyperplane of r -dimensions, we retain the first r principal components from the PCA transformation. For our case, we will use 3-dimensional data to fit a 1-dimensional hyperplane (a line) and project that line back into 3-space. So, we will retain the first principal component from the PCA analysis.

MATLAB has a built in algorithm to perform the principal components analysis and return the principal components. We use this algorithm on our matrix of coordinates to get the first principal

components, which is the direction vector for our line in space, corresponding to the coefficients k_x, k_y, k_z in Equation 3.9. t will range from the minimum score to the maximum score returned from the PCA algorithm. Then, x_0, y_0, z_0 are the means of the values of the corresponding coordinate.

Figure 3.3: Example PCA Orthogonal Regression



The results from an example principal components analysis is shown in Figure 3.3. The circles are the LMA points and the line is the resultant orthogonal best fit line. It's not entirely obvious because this picture is a 2d print of a 3d image, but one can tell that the line looks like it is very close to fitting all of the data.

We have developed all of the mechanics and theory behind the line charge model. In practice, the computation is performed by a MATLAB program that imports LMA data and $\Delta \vec{E}$ field mill data for a given flash from text files, then creates images of those LMA source points below the Earth's conducting surface. Then, the program performs principal components analysis on the LMA

source points to get the parameters for the charge distributions' orthogonal best fit line. Then, we numerically integrate Equation 3.12 for each line and each field mill. These results are placed into a matrix like A in Equation 3.16. Then MATLAB solves Equation 3.16 with appropriate constraints for Q . First, the positive distributions must have a $Q > 0$. Similarly, the negative distributions must have $Q < 0$. If the flash is IC, charge is conserved, so the total charge from all positive distributions and the total charge from all negative distributions will be zero. Or, $Q_+ + Q_- = 0$. If the flash is CG, then the model will converge on the best solution not constrained such that $Q_+ + Q_- = 0$, and the difference between Q_+ and Q_- is the charge transferred to the ground. For further instruction on operating the program, consult the appendix.

Chapter 4

Model Verification

In this Chapter we will offer evidence that the assumptions of our model match physical reality and are in agreement with previous investigations into lightning charge transfer.

First, we want to ensure that Equation 3.12 actually represents a constant that when multiplied by charge Q , returns the z-component of electric field due to a line of charge in an arbitrary configuration in space. To show this equation holds, we first point to the electromagnetic theory expounded in the previous chapter. Equation 3.12 conforms with the background theory, especially Coulomb's Law, which it is derived from.

But, to provide us with greater certainty, we ran a series of computational experiments comparing electric fields due to lines with different configurations in space to the electric field due to a large number of small point charges placed along the same line. So we randomly picked coefficients $k_x, k_y, k_z, x_0, y_0, z_0, t_i, t_f$ for Equation 3.9. We assumed that this represents a line of charge in space with charge of 1 Coulomb. Then, we ran a program in Python that calculates the electric field due to a large number N point charges along the path of the line defined by Equation 3.9. So, each tiny point charge had a charge of $1/N$ Coulombs and a position, defined recursively at each point by the following set of equations:

$$t_i \leq t \leq t_f \quad (4.1)$$

$$\vec{r}_1' = (k_x t_i + x_0)\hat{x} + (k_y t_i + y_0)\hat{y} + (k_z t_i + z_0)\hat{z} \quad (4.2)$$

$$\vec{r}_n' = (k_x(t_{n-1} + \Delta t) + x_0)\hat{x} + (k_y(t_{n-1} + \Delta t) + y_0)\hat{y} + (k_z(t_{n-1} + \Delta t) + z_0)\hat{z} \quad (4.3)$$

$$\Delta t = \frac{t_f - t_i}{N} \quad (4.4)$$

So we can find the z-component of the electric field at the point $\vec{r} = 0\hat{x} + 0\hat{y} + 0\hat{z}$ due to the n th point charge with a total charge of $Q = 1\text{C}$ by plugging the above equation into Equation 3.2. So,

$$\vec{E}_{zn} = \frac{1}{4\pi\epsilon_0} \frac{(1/N)(-(k_z(t_{n-1} + \Delta t) + z_0))}{|-r_n'|^3} \quad (4.5)$$

We get the total electric field E_z by adding up all the tiny electric fields from E_1 to E_N . Next, we can input the parameters $k_x, k_y, k_z, x_0, y_0, z_0, t_i, t_f$ into our MATLAB code for the model, and solve Equation 3.12 by solving the integral.

The first problem we should tackle is to try to find the electric field due to a line of charge placed on the x-axis, with charge of $Q = 1\text{ C}$. This was explored earlier in the paper, in Section 3.1. The electric field due to the line is given by Equation 3.7. We let the line range from -10 meters to +10 meters on the x-axis, or from (-10, 0) to (10, 0). Then we choose the point where we measure the field to be at (0, 10). Using these values with Equation 3.7, we find that $\vec{E} = 6.364 \times 10^7 \text{ V m}^{-1}$. Then, the result from integrating Equation 3.12 is $\vec{E} = 6.36396 \times 10^7 \text{ V m}^{-1}$. Then iterating over 50000 tiny point charges using Equation 4.5, $\vec{E} = 6.36397 \times 10^7 \text{ V m}^{-1}$. These values are almost exactly the same.

Table 4.1 compares charge transfer results between the line charge model and the Maggio distributed charge model in Maggio [2007]. We have access to the complete Maggio data set, including LMA source points for each charge distribution in each flash and $\Delta\vec{E}$ field mill measurements for each flash. The results from the Maggio Distributed Charge Model are reported under "Distributed Charge Region" and the results from the line charge model are found below "Line Charge." Both figures are reported in Coulombs. Flashes are identified by the UTC time that they occurred, over

the range of dates 7/25/99 to 8/7/99. The percent difference between the two values is reported to the right. The modeled electric fields are the electric fields resulting from either the lines of charge with the final charge result Q of appropriate polarity or the electric field resulting from a charge of Q/N of appropriate polarity on N LMA points in accordance with the Maggio distributed charge model. Ideally, the modeled electric fields would be as close as possible to the measured electric fields.

Table 4.1: Simulation Comparison Data.

Flash 2134:57 UTC	IC Flash		
	Line Charge Model:	Distributed Charge Model:	Percent Difference:
	7.13 C	8.40 C	16%
	Modeled E-Fields:	Field Mill Station:	Measured E-Fields:
	-3000.84 V/m	-3137.40 V/m	1 -3000.00 V/m
	-1965.82 V/m	-2169.40 V/m	2 -1900.00 V/m
	-3259.53 V/m	-3540.50 V/m	3 -3300.00 V/m
Flash 2135:21 UTC	IC Flash		
	Line Charge Model:	Distributed Charge Model:	Percent Difference:
	11.10 C	9.20 C	19%
	Modeled E-Fields	Field Mill Station:	Measured E-Fields:
	-2910.80 V/m	-2239.00 V/m	1 -2700.00 V/m
	-1260.30 V/m	-1426.00 V/m	2 -1800.00 V/m
	2526.30 V/m	-2465.00 V/m	3 -2500.00 V/m
Flash 2138:39 UTC	IC Flash		
	Line Charge Model	Distributed Charge Model:	Percent Difference:
	6.75 C	7.00 C	4%
	Modeled E-Fields:	Field Mill Station:	Measured E-Fields:
	-5332.00 V/m	-5463.00 V/m	1 -5700.00 V/m

-5017.00 V/m	-5248.00 V/m	2	-5000.00 V/m
-6488.00 V/m	-6632.00 V/m	3	-6200.00 V/m

Flash 2149:49 UTC	IC Flash		
Line Charge Model:	Distributed Charge Model:		Percent Difference:
19.50 C	20.80 C		6%
Modeled E-Fields:		Field Mill Station:	Measured E-Fields:
-7698.00 V/m	-8753.00 V/m	1	-9000.00 V/m
-10092.00 V/m	-10212.00 V/m	2	-9100.00 V/m

Flash 2153:11 UTC	IC Flash		
Line Charge Model:	Distributed Charge Model:		Percent Difference:
12.90 C	12.30 C		5%
Modeled E-Fields		Field Mill Station:	Measured E-Fields:
-2614.00 V/m	-2101.00 V/m	1	-2500.00 V/m
-3103.00 V/m	-3239.00 V/m	2	-3200.00 V/m

Flash 2158:49 UTC	IC Flash		
Line Charge Model:	Distributed Charge Model:		Percent Difference:
20.57 C	27.70 C		30%
Modeled E-Fields:		Field Mill Station:	Measured E-Fields:
-5178.00 V/m	-5108.00 V/m	1	-4100.00 V/m
-4156.00 V/m	-4975.00 V/m	2	-5500.00 V/m

Flash 1944:00 UTC	CG Flash		
-------------------	----------	--	--

	Line Charge Model:	Distributed Charge Model:		Percent Difference:
	10.33 C	11.50 C	Q to Ground	11%
	Modeled E-Fields:		Field Mill Station:	Measured E-Fields:
	-4048.00 V/m	-4734.00 V/m	1	-4900.00 V/m
	-4024.00 V/m	-3429.00 V/m	2	-4100.00 V/m
	-5841.00 V/m	-6494.00 V/m	3	-5200.00 V/m

Flash 1946:55 UTC	IC Flash			
	Line Charge Model:	Distributed Charge Model:		Percent Difference:
	10.96 C	10.60 C		3%
	Modeled E-Fields:		Field Mill Station:	Measured E-Fields:
	-1802.00 V/m	-1888.00 V/m	1	-2500.00 V/m
	-4527.00 V/m	-4602.00 V/m	2	-4100.00 V/m
	-3188.00 V/m	-3281.00 V/m	3	-3400.00 V/m

Flash 2247:46 UTC	IC Flash			
	Line Charge Model:	Distributed Charge Model:		Percent Difference:
	3.76 C	3.90 C		4%
	Modeled E-Fields		Field Mill Station:	Measured E-Fields:
	-1904.00 V/m	-1915.00 V/m	1	-1900.00 V/m
	-439.00 V/m	-375.40 V/m	2	-400.00 V/m
	-871.00 V/m	-821.00 V/m	3	-900.00 V/m

Flash 2248:52 UTC	IC Flash			
	Line Charge Model:	Distributed Charge Model:		Percent Difference:
	4.88 C	4.40 C		10%
	Modeled E-Fields:		Field Mill Station:	Measured E-Fields:
	-1240.00 V/m	-1136.00 V/m	1	-1500.00 V/m

-1154.00 V/m	-999.70 V/m	2	-800.00 V/m
-1122.00 V/m	-1017.00 V/m	3	-1200.00 V/m

Flash 2249:16 UTC	IC Flash		
Line Charge Model:	Distributed Charge Model:		Percent Difference:
14.83 C	12.60 C		16%
Modeled E-Fields:		Field Mill Station:	Measured E-Fields:
-4102.00 V/m	-3956.00 V/m	1	-3400.00 V/m
-2397.00 V/m	-2468.00 V/m	2	-2400.00 V/m
-2755.00 V/m	-3002.00 V/m	3	-3800.00 V/m
Flash 2250:05 UTC	IC Flash		
Line Charge Model:	Distributed Charge Model:		Percent Difference:
5.97 C	5.40 C		10%
Modeled E-Fields:		Field Mill Station:	Measured E-Fields:
-2586.00 V/m	-2381.00 V/m	1	-2600.00 V/m
-1555.00 V/m	-1628.00 V/m	2	-1500.00 V/m
-1973.00 V/m	-1955.00 V/m	3	-2000.00 V/m
Flash 2250:23 UTC	IC Flash		
Line Charge Model:	Distributed Charge Model:		Percent Difference:
7.89 C	8.20 C		4%
Modeled E-Fields:		Field Mill Station:	Measured E-Fields:
-4287.00 V/m	-4038.00 V/m	1	-4900.00 V/m
-3138.00 V/m	-3538.00 V/m	2	-2900.00 V/m
-4152.00 V/m	-4027.00 V/m	3	-3700.00 V/m
Flash 2250:45 UTC	IC Flash		
Line Charge Model:	Distributed Charge Model:		Percent Difference:

	7.47 C	9.60 C		25%
	Modeled E-Fields:		Field Mill Station:	Measured E-Fields:
	-2432.00 V/m	-2397.00 V/m	1	-2500.00 V/m
	-2137.00 V/m	-2158.00 V/m	2	-2000.00 V/m
	-2242.00 V/m	-2160.00 V/m	3	-2300.00 V/m
<hr/>				
Flash 2019:59 UTC	CG Flash			
	Line Charge Model:	Distributed Charge Model:		Percent Difference:
	4.42 C	7.00 C	Q to Ground	45%
	Modeled E-Fields:		Field Mill Station:	Measured E-Fields:
	-3500.00 V/m	-3576.00 V/m	1	-3500.00 V/m
	-2500.00 V/m	-2424.00 V/m	3	-2500.00 V/m
<hr/>				
Flash 2016:26 UTC	IC Flash			
	Line Charge Model:	Distributed Charge Model:		Percent Difference
	7.54 C	8.90 C		17%
	Modeled E-Fields:		Field Mill Station	Measured E-Fields:
	-2656.00 V/m	-2826.00 V/m	1	-2900.00 V/m
	-3879.00 V/m	-4114.00 V/m	2	-3500.00 V/m
	-4098.00 V/m	-4401.00 V/m	3	-4300.00 V/m

We find that 9 out of 16 of the above flashes have a percent difference in calculated charge transfer of 10 percent or less. This implies a majority of the flashes have a very close fit when modeled by either the distributed charge model or the line charge model. Flashes with percent differences of over 10 percent are less close, but note that there are no outlandish numbers or extreme outliers. We conclude that the line charge model is in close accordance with the distributed charge model, for CG and IC flashes.

Because the model produces a result in accordance with electromagnetic theory and in accordance

with a previous model, we claim that the model will produce reliable results when analyzing new lightning flashes.

Chapter 5

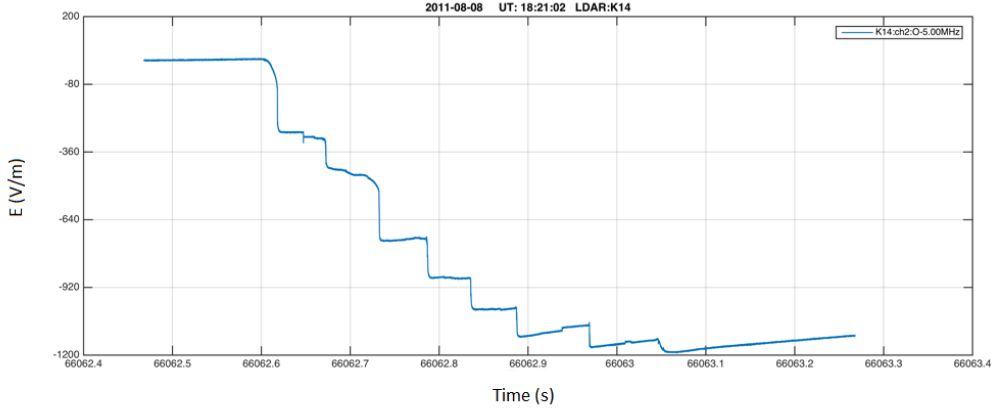
Analysis of Individual Return Strokes

Cloud to ground flashes are typically accompanied with one or more connections to the ground [Rakov and Uman, 2003]. The successive connections to ground are accompanied with a deposition of electric charge, and are called return strokes. Each return stroke corresponds with a quick, abrupt rearrangement of charge, and as such can be analyzed with the above techniques, given instruments which measure the electric field at a high enough resolution that one can resolve the change in electric field due to each individual return stroke. The slow antenna (discussed in Section 2.3) has sufficient resolution to view each electric field drop due to each return stroke. Figure 5.1 is a plot of the Electric Field vs. time for Flash 18:21:03 on August 8, 2011, analyzed by Conn [2012].

Each sharp jump down on the plot is a result the change in electric field after rearrangement of charge in each individual return stroke. One can count eight sharp drops in electric field, so this CG flash produced eight return strokes. The quantity of eight return strokes was further corroborated with video footage of the flash. Conn's analysis, using the Maggio Distributed Model, found a total charge transfer of 50.2 C to ground, involving three distinct charge regions as determined by LDAR data. The analysis used 30 values for electric field change from electric field mills at KSC.

We re-simulated this flash overall using similar electric field mill readings and LDAR sources, but

Figure 5.1: Electric Field Determined by Slow Antenna, at KSC Mill 14



using eight line charges corresponding to LDAR sources originating from each of the eight return strokes, rather than three distributed charge regions. Overall, the re-simulation returned that a total charge of 49.46 C was transferred to ground. This is a percent difference of 1.5% compared to the analysis by Conn [2012].

Slow antenna data were obtained for the flash for three flat plate antennas. The net charge transfer of each return stroke could be determined by finding the change in electric field after each return stroke, then running the simulation with those LDAR source points that correspond to the return stroke. The results from the analysis are presented in Table 5.1, along with the error between the measured and modeled electric fields at the three flat plate antennas. When we added the charge transferred in each return stroke, we found a total charge transfer of 58.97 C. This value should be very close to the value obtained by looking at the flash as a whole, 49.46 C. These values have a percent difference of 17.5%.

Table 5.1: Results of Individual Return Stroke Analysis

Return Stroke	Charge Transferred to Ground
1	14.79 C
2	14.05 C
3	10.5 C
4	5.25 C
5	3.966 C
6	3.70 C
7	2.99 C
8	3.73 C
Total	58.97 C

Chapter 6

Conclusion

Experiments attempting to quantify electric charge transfer in lightning flashes have been ongoing for a century. This investigation employed a model that treats the regions where we assume charge is being deposited as continuous lines of charge. When we performed this analysis on flashes that were analyzed with a previous model, the results were very similar. The net charge transfer of a majority of the flashes analyzed were within 10% of the previous model. Also, this analysis was performed on a Florida CG flash, and the result was 1.5% different from the previously determined value for the overall flash. We then analyzed the Florida CG flash by its individual return strokes, finding a total charge transfer (by adding the charge transferred in each return stroke) of 58.97 C. This is relatively close to the analysis of the flash as a whole, with a percent difference of 17.5%.

This implies that the line charge model is prepared to provide further insight into phenomena arising in atmospheric electricity. Future work may include analysis like that presented above, where we find total charge transfer in IC and CG flashes, as well as individual return strokes in CG flashes. The analysis of these flashes might be applied to more phenomena that arise in atmospheric electricity, such as estimations of the energy released in lightning flashes or insight into the Global Electric Circuit, which is the movement of electric charge between the earth's surface and the ionosphere. Applications abound, and the line charge model provides a new framework to begin investigations to reveal insights into these applications.

Bibliography

- C. Conn. *Charge transfer analysis of Florida lightning flashes*. Undergraduate research prospectus, Mississippi College, 2012.
- D. Griffiths. *Introduction to Electrodynamics*. Pearson, 4th edition, 2012.
- E. A. Jacobson and E. P. Krider. Electrostatic field changes produced by florida lightning. *Journal of the Atmospheric Sciences*, 33(1):103–117, 1976. doi: 10.1175/1520-0469(1976)033<0103:efcpbf>2.0.co;2.
- W. J. Koshak, E. P. Krider, N. Murray, and D. J. Boccippio. Lightning charge retrievals: Dimensional reduction, lidar constraints, and a first comparison with lis satellite data. *Journal of Atmospheric and Oceanic Technology*, 24(11):1817–1838, 2007. doi: 10.1175/jtech2089.1.
- C. R. Maggio. *Estimations of lightning charge transfers in New Mexico thunderstorms, and applications to lightning energy, thunderstorm generator currents and above-cloud transient currents*. PhD thesis, University of Mississippi, 2007.
- T. Masson. *Estimations of the Electric Charge Transferred by Two Intracloud Lightning Flashes Occurring Over Central Florida During the Summer of 2011*. Undergraduate honors thesis, Mississippi College, 2014.
- Mathworks. Fitting an orthogonal regression using principal components analysis, 2015. <https://www.mathworks.com/help/stats/examples/fitting-an-orthogonal-regression-using-principal-components-analysis.html>.
- V. A. Rakov and M. A. Uman. *Lightning: Physics and Effects*. Cambridge University Press, 2003.

- S. E. Reynolds and H. W. Neill. The distribution and discharge of thunderstorm charge-centers. *Journal of Meteorology*, 12(1):1–12, 1955.
- W. Rison, R. J. Thomas, P. R. Krehbiel, T. Hamlin, and J. Harlin. A gps-based three-dimensional lightning mapping system: Initial observations in central new mexico. *Geophysical Research Letters*, 26(23):3573–3576, Jan 1999. doi: 10.1029/1999gl010856.
- X. M. Shao and P. R. Krehbiel. The spatial and temporal development of intracloud lightning. *Journal of Geophysical Research: Atmospheres*, 101(D21):26641–26668, Jan 1996. doi: 10.1029/96jd01803.
- R. G. Sonnenfeld, J. D. Battles, G. Lu, and W. P. Winn. Comparing efield changes aloft to lightning mapping data. *Journal of Geophysical Research*, 111(D20), 2006. doi: 10.1029/2006jd007242.
- M. Stolzenburg, W. D. Rust, B. F. Smull, and T. C. Marshall. Electrical structure in thunderstorm convective regions: 3. synthesis. *Journal of Geophysical Research: Atmospheres*, 103(D12):14059–14078, Jan 1998. doi: 10.1029/97jd03546.
- L. Vickers. *Estimation of Charge Transfers by Individual Lightning Return Strokes*. Undergraduate honors thesis, Univeristy of Mississippi, 2010.
- C. T. R. Wilson. On some determinations of the sign and magnitude of electric discharges in lightning flashes. *Proceedings of the Royal Society A: Mathematical, Physical and Engineering Sciences*, 92(644):555–574, Jan 1916. doi: 10.1098/rspa.1916.0040.

Chapter 7

Appendix - Instructions for Operating the Program

The model was originally programmed using MATLAB 2015a. One Python script, originally programmed in Python 3 with Numpy and Scipy, is used for formatting the inputs required for the program. The current source code repository is https://github.com/williamrhawkins/lightning_line_charges, and currently contains all of the MATLAB source code, the Python script `format_LMA_sources.py`, re-simulations of the flashes in Maggio [2007], and initial re-simulations of the flash in Conn [2012].

In the Source directory, `LCD_MAIN.m` is the main file that is executed to run the program. `integral.m` and `princom.m` are files containing functions that are called by `LCD_MAIN.m`. `integral.m` handles the integration and `princom` handles the principal components analysis. `field.txt` is edited for each flash to contain the electric field values at each field mill. `mills.txt` contains coordinates for all of the KSC field mills (1 through 34) and the three field mills at Langmuir Lab (35, 36, 37). 35 references the Annex mill, 36 refers to the Kiva mill, and 37 refers to the Hangar mill.

In order to operate the program, you must have a number of measured electric field values, the field mill's numbers for the electric field values, and `.txt` output from the Lightning Tracker program for LMA/LDAR sources. The first operation is formatting the `.txt` Lightning Tracker output to a format that MATLAB can read. The user will run `format_LMA_sources.py`, type in the

filename of the .txt Lightning Tracker output, press enter, then type the name of the output file. The output file must be saved as “pos1.txt”, “neg1.txt”, “pos2.txt”, “neg2.txt”, and similarly. The MATLAB program reads in files of LMA/LDAR source points with “pos” or “neg”, then a number corresponding to the number that refers to that charge region. Once all of the LMA/LDAR source files are converted to a file with “negN.txt” or “posN.txt”, copy all of those files into the program’s Source directory.

Now, we must input values for the measured electric field drops at each field mill. Open the file Source/field.txt with a text editor. Now, enter in the measured electric fields, one per line. Include the sign with the field value. When we enter the field mills we are using into the program later, the first electric field value will correspond to the first field mill entered into the program, and the rest follow in the order that they are entered.

At this point, we can execute LCD_MAIN.m in MATLAB. The first prompt will say “Enter the number of negative distributions.” Here, enter the number of negative distributions. There must be the same number of “negN.txt” .txt files with LMA/LDAR source points as there are negative distributions. Next, we are prompted “Enter the number of positive distributions.” Do the same for the positives. Now, we are asked if the flash is intracloud. Enter 1 if the flash is intracloud so the program will search for a solution that conserves charge in the cloud. Enter 0 if the flash is cloud-to-ground.

Next, the program prompts us for the numbers of the field mills to use. Here, we can use MATLAB notation to refer to a range of mills. If we want mills 1-20, we enter “1:20”. If there is a gap in the range, separate with a space: for field mills 1-5, 7-15, and 22, we would enter “1:5 7:15 22”. The KSC mills are numbered with their typical number, 1-34, and the Langmuir Lab mills are 35 through 37.

Once the field mills are entered, the program will begin importing the required data and performing computations. The final result is reported in a file called “out.txt”, which contains the estimated charge placed on each of the positive lines, then the negative lines, and then the net transfer if the charge is CG. After that, the modeled electric fields and the residual electric fields (the error between the modeled electric fields and the measured electric fields) are displayed. With practice, the user can get in the routine of setting up the program to analyze a flash fairly easily.

On my 4 core Intel i7 machine, the program runs quickly, analyzing CG flashes with 30 field mills and 8 charge distributions in a few seconds.

Biographical Sketch of the Author

William Rabon Hawkins is a senior Physics and Mathematics student from Cleveland, Mississippi. He began studies at Mississippi College in Fall 2013, and will graduate in May 2017. He began his research on models for estimating electric charge transfer in lightning flashes, advised by Dr. Chris Maggio, in Spring 2016, and completed the honors thesis in Spring 2017.

While studying at Mississippi College, William served as a summer intern at the US Army Engineer Research and Development Center, where he completed research on simulated transient thermal infrared emissions of forest canopies during rainfall events. His presentation at the 2017 Meeting of the LA/MS Section of the Mathematical Association of America, “Zeckendorf’s Theorem and Fibonacci Coding,” received second place in the undergraduate papers competition. William is a member of Mortar Board, Pi Mu Epsilon, and Alpha Chi. He received the Senior Mathematics Award and the Perry Academic Award. When not working on math problems, William enjoys making coffee, playing soccer, watching baseball, and reading. After graduation, he will begin the Ph.D. in Applied Mathematics at North Carolina State University.